8-4-2015

The pH Low Insertion Peptide pHLIP Variant 3 as a Novel Marker of Acidic Malignant Lesions

Thomas T. Tapmeier

Anna Moshnikova
University of Rhode Island, a_moshnikova@uri.edu

John Beech

Danny Allen

Paul Kinchesh

See next page for additional authors

Follow this and additional works at: https://digitalcommons.uri.edu/phys_facpubs

Authors

Thomas T. Tapmeier, Anna Moshnikova, John Beech, Danny Allen, Paul Kinchesh, Sean Smart, Adrian Harris, Alan McIntyre, Donald M. Engelman, Oleg A. Andreev, Yana K. Reshetnyak, and Ruth J. Muschel

The pH low insertion peptide pHLIP Variant 3 as a novel marker of acidic malignant lesions

Thomas T. Tapmeier[a], Anna Moshnikova[b], John Beech[a], Danny Allen[a], Paul Kinchesh[a], Sean Smart[a], Adrian Harris[c], Alan McIntyre[c,d], Donald M. Engelman[e,1], Oleg A. Andreev[b], Yana K. Reshetnyak[b], and Ruth J. Muschel[a,1]

[a]Cancer Research UK and Medical Research Council Oxford Institute for Radiation Oncology and Biology, Department of Oncology, University of Oxford, Oxford OX3 7DQ, United Kingdom; [b]Physics Department, University of Rhode Island, Kingston, RI 02881; [c]Weatherall Institute of Molecular Medicine, Department of Oncology, University of Oxford, Oxford OX3 9DS, United Kingdom; [d]Cancer Biology, Division of Cancer and Stem Cells, University of Nottingham, Queen's Medical Centre, Nottingham NG7 2UH, United Kingdom; and [e]Department of Molecular Biophysics and Biochemistry, Yale University, New Haven, CT 06520

Current strategies for early detection of breast and other cancers are limited in part because some lesions identified as potentially malignant do not develop into aggressive tumors. Acid pH has been suggested as a key characteristic of aggressive tumors that might distinguish aggressive lesions from more indolent pathology. We therefore investigated the novel class of molecules, pH low insertion peptides (pHLIPs), as markers of low pH in tumor allografts and of malignant lesions in a mouse model of spontaneous breast cancer, BALB/neu-T. pHLIP Variant 3 (Var3) conjugated with fluorescent Alexa546 was shown to insert into tumor spheroids in a sequence-specific manner. Its signal reflected pH in murine tumors. It was induced by carbonic anhydrase IX (CAIX) overexpression and inhibited by acetazolamide (AZA) administration. By using ^{31}P magnetic resonance spectroscopy (MRS), we demonstrated that pHLIP Var3 was retained in tumors of pH equal to or less than 6.7 but not in tissues of higher pH. In BALB/neu-T mice at different stages of the disease, the fluorescent signal from pHLIP Var3 marked cancerous lesions with a very low false-positive rate. However, only ~60% of the smallest lesions retained a pHLIP Var3 signal, suggesting heterogeneity in pH. Taken together, these results show that pHLIP can identify regions of lower pH, allowing for its development as a theranostic tool for clinical applications.

in vivo fluorescence | carbonic anhydrase IX | pHLIP | invasive tumor | early detection

The reprogramming of metabolism resulting in enhanced glycolysis is now a well-recognized characteristic of many cancers. Increased levels of glycolysis—while contributing to energy generation—are essential to supply carbon backbones for the synthesis of the nucleotides required to sustain DNA synthesis under conditions of abnormal proliferation (1, 2). Thus, the well-recognized Warburg effect plays a physiological role in sustaining the malignant phenotype. In addition to the requirement for nucleotide synthesis, glycolysis can be essential for energetics under hypoxia. Because a poor vascular supply is also characteristic of cancers, hypoxia generated by poor perfusion is now regarded as a hallmark of cancer (3). This hypoxia, if sufficiently extreme, may dictate that cancer cells as well as macrophages and other stromal cells in the hypoxic microenvironment use glycolysis to maintain bioenergetics. It has recently been established that endothelial cells participating in sprouting angiogenesis rely on glycolysis for their energy requirements (4). Furthermore, many of the most prevalent and well-known oncogenic signaling pathways such as myc and PI3K redirect the cancer cell metabolism toward increased glycolysis (1, 2). Thus, levels of glycolysis greater than those found in normal tissues are associated with malignancy.

One consequence of glycolysis is the production and secretion of lactate, resulting in decreased extracellular pH (5, 6). In addition, cancer cells and especially hypoxic cancer cells express carbonic anhydrases IX and XII (7, 8), which catalyze the formation of extracellular acid from carbon dioxide and thus enhance acidic extracellular pH (9). Extracellular acidity as evoked by tumor progression has the potential to regulate multiple biological processes such as proliferation, angiogenesis, immunosuppression, invasion, and chemoresistance (5, 10–16). Exposure of cancer cell lines to acidic pH (6.8) increased migration and invasion in vitro (17) and in vivo (18). Acidic pH induces increased expression and release of MMP-9 (19) and MMP-2 (18). Reduction of tumor pH by oral bicarbonate treatment reduced metastasis in vivo in xenografts (20). Thus, alterations in extracellular pH are characteristic of cancer and are thought to contribute to aspects of the malignant phenotype and to resistance to some forms of therapy.

Cancer rarely arises in a single step but instead represents a series of genetic alterations, eventually leading to fully formed tumors. At the pathological level, this can be seen as lesions first showing hyperproliferation, and dysplasia followed by invasion. This process can be accelerated in mice bearing transgenes that already have genetic alterations that predispose them to cancer. Accordingly, we wished to ask whether detection of acid pH in a tumor might be a useful biomarker for detection of early neoplasia.

Because the extracellular pH in tumors is just 0.5–1 pH units lower than the extracellular pH in normal tissue, it has proven challenging to design molecular probes sensitive to this difference. Several magnetic resonance (MR)-based approaches to measure tumor acidity have been developed (21), all with some significant limitations in regards to translation to the clinic. Although a number of pH-sensitive tumor-targeting agents have

Significance

Acidic pH may distinguish aggressive from more indolent cancers. The limitation on testing this hypothesis to date has been the difficulty of measuring acidic pH in cancers. Here we show that retention of the pH low insertion peptide (pHLIP) Variant 3 (Var3) reflects acidic pH. Using pHLIP Var3, we show its ability to detect cancer with a low false-positive rate in a genetically engineered model of murine breast cancer, paving the way for testing this probe in clinical situations.

been recently introduced (22, 23), the challenge has been to achieve fast pH transition within a single pH unit, to discriminate healthy tissue of normal pH from the more acidic environment of tumors.

A novel class of molecules that target areas of low pH has recently been developed: the pH low insertion peptides (pHLIPs) (24). The mechanism of pHLIP-mediated targeting is based on pH-dependent membrane-associated folding into a coil conformation, which releases free energy (25). This coil inserts into cell membranes and thus allows selective targeting of cancerous tissue of low extracellular pH (pH 6.0–6.8) while avoiding retention in healthy tissue (pH 7.2–7.4). WT-pHLIP has been successfully tested in vitro as an agent for intracellular delivery of large polar cargo molecules (26–29). In addition, WT-pHLIP promotes pH-dependent fusion of pHLIP-coated liposomes containing gramicidin channels with cellular membranes, thus destroying the balance of monovalent ions (30).

In vivo, pHLIP has been used as a marker in mouse models of cancer (31–38), ischemia (39), arthritis (33), and influenza (40). It also has been used to target various nanoparticles (41, 42) (43) and liposomes (39, 44) to acidic tissue. Studies differ as to whether the actual pH was determined by ^{31}P magnetic resonance spectroscopy (MRS) (32, 34, 38) or other methods (45). Tumor pH alteration has been attempted by bicarbonate (34) or carbonic anhydrase IX (CAIX) overexpression (38), and the effect on pHLIP uptake has been registered.

Clinical applications have focused on the topical application of pHLIP onto biopsies from human head and neck cancer patients, where pHLIP detected cancerous tissue within the samples (46, 47).

However, no systematic assessment of the degree of pHLIP labeling in regard to pathological findings had been undertaken, which is now the main focus of our study. Most of the examples above used WT-pHLIP for their studies. We compared uptake with pHLIP Variant 3 (Var3) and Var7, as these had previously been selected among 16 rationally designed pHLIP variants as the best potential tumor-targeting pHLIPs (24). These data led us to concentrate our efforts on pHLIP Var3, recently introduced as an optimized tumor-targeting pHLIP (24), to correlate its tumor uptake and retention with (i) tumor pH and (ii) manipulation of extracellular pH by CAIX overexpression and inhibition through acetazolamide (AZA) and (iii) evaluate Var3 use under "clinical" conditions for targeting of early and developed lesions using the spontaneous breast cancer model BALB/neu-T (48) as it progresses from atypical hyperplasia to invasive carcinomas.

Results

First we used 4T1 breast cancer cells, which closely mimic triple-negative human breast cancer, grown as allografts in BALB/c mice to assess targeting and retention of fluorescent pHLIPs. pHLIP variants Var3 and Var7 (Table 1) and their corresponding nontargeting K-pHLIP controls, all conjugated with Alexa546,

Fig. 1. Comparison of uptake and retention of pHLIP variants in vivo. Tumors from the 4T1 cell line were grown in syngeneic BALB/c mice. Once the tumors reached a GMD of 5 mm, different pHLIP variants (n = 5 per group) were injected intravenously. Fluorescence was normalized to the initial signal before pHLIP injection. (A) Tumor growth with time after inoculation. Uptake of pHLIPs Var3 and (B) K-Var3 Var7 and K-Var7 (C) followed by in vivo fluorescence over time (data are mean ± SEM).

were administered by tail vein injection once 4T1 tumors reached 5 mm in geometric mean diameter (GMD; Fig. 1A). Increased fluorescence in the tumors was observed 1 h after injection, with a further increase of the signal over 5 h (Fig. 1 B and C). Fluorescence still persisted after 24 h. pHLIP Var3 had enhanced tumor targeting and greater retention than pHLIP Var7. To account for irregular tumor vasculature as a possible cause for pHLIP retention, we compared pHLIP Var3 and Var7 to their noninserting counterparts K-Var3 and K-Var7 (Table 1). Although injection of the K-pHLIPs led to an increase in fluorescence above background over 24 h (~250%), fluorescence from pHLIP Var3 and Var7 was 5–10-fold as high, indicating a significant contribution of low pH targeting. Because pHLIP Var3 showed the most persistent fluorescence signal and retention, further experiments were conducted with pHLIP Var3.

Using spheroids as a tissue culture 3D model for tumors, the uptake of pHLIP Var3 and of the K-pHLIP noninserting control peptide was compared between spheroids with different levels of extracellular acidity. We used the cell line HCT116, reported both to have low expression of CAIX and to readily form spheroids (8), and HCT116 transduced to overexpress CAIX, leading to acidification of the extracellular space (8) (Fig. 2 A and B). As expected, the CAIX-overexpressing spheroids, generating more acid, grew faster than the empty vector (EV) controls (Fig. S1A) and were targeted by pHLIP Var3 better than EV spheroids. We also compared the K-pHLIP Var3 control with pHLIP Var3 within the same spheroid by tagging them to different fluorochromes (Var3-Alexa546 and K-Var3–Alexa647; Fig. 2C). pHLIP Var3 was detected throughout the spheroid, whereas K-pHLIP Var3 remained on the outside. Thus, the uptake and retention of pHLIP Var3 was sequence-specific and pH-responsive.

Next, we tested whether pHLIP Var3 retention in tumors in vivo was altered by CAIX overexpression (Fig. 3). As reported (8), the growth rate of tumors from CAIX-overexpressing cells (HCT116 CAIX) was greater than that of the controls (HCT116 EV; Fig. 3A). We normalized the fluorescence of pHLIP Var3 to tumor volume. The CAIX-overexpressing tumors (Fig. S1B) had a significantly higher uptake of pHLIP Var3 than the controls at both 5 h and 18 h (Fig. 3B). To establish that pHLIP Var3 uptake by tumors reflected extracellular acid pH, we asked whether inhibition of CAIX activity by AZA (49) would reduce uptake or retention of Var3 within tumors. We injected mice bearing 4T1 tumors with AZA (40 mg/kg, i.p.) followed by injection of pHLIP Var3 24 h later (Fig. 3C). The fluorescence signal from the pHLIP Var3 probe was monitored over another 24 h. The mice treated with AZA showed a significantly greater decline in the fluorescence signal compared with untreated controls. This indicates that pHLIP Var3 retention indeed correlates with the extracellular pH of tumors, that changes in tumor pH will be

Table 1. The amino acid sequence of the pHLIP variants and K-pHLIP controls

Probe	Amino acid sequence
WT	ACEQNPIYWARYADWLFTTPLLLLDLALLVDADEGT
Var3	ACDDQNPWRAYLDLLFPTDTLLLDLLW
Var7	ACEEQNPWARYLEWLFPTETLLLEL
K-Var3	ACDDQNPWRAYLKLLFPTKTLLLKLLW
K-Var7	ACEEQNPWARYLKWLFPTKTLLLKL

The transmembrane protonatable D and E (underlined) residues in Var3 and Var7 were replaced by positively-charged K residues (also underlined) in K-Var3 and K-Var7, which prevents K-Var insertion into membrane and thus tumor targeting.
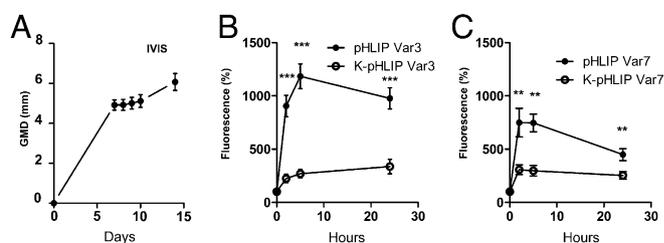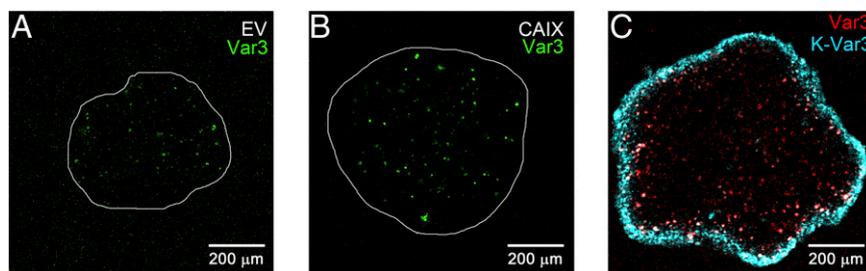
Fig. 2. The ability of pHLIP to penetrate the spheroid is sequence specific. (*A* and *B*) Following incubation with fluorescent pHLIP Var3 for 6 h, pHLIP fluorescence in HCT116 spheroids was recorded from equatorial sections in a confocal microscope (magnification, 200×). Within 3 d, the CAIX-overexpressing spheroids (*B*) grew larger than the EV ones (*A*). (*C*) Staining of CAIX-overexpressing spheroids with both Var3 (red) and control peptide K-Var3 (blue) showed that Var3 was retained within the spheroid, whereas K-Var3 was not taken up and remained outside.

reflected by changes in pHLIP Var3 signal, and that protein levels of CAIX do not directly affect pHLIP Var3 retention.

Finally, we attempted to establish a direct correlation of actual pH within the tumor to pHLIP Var3 uptake and retention in vivo. To determine the pH of tumors, we used the ^{31}P MRS method (50). We used inorganic phosphate, phosphocreatine (PCr), and ATP to calculate the overall pH from MRS spectra (Table S1). According to the literature, approx. 70% of the signal in bulk pH measurement is from intracellular sources and 30% from extracellular ones. Hence, a large enough difference in extracellular pH would still be reflected in the signal (50–52). To avoid contamination of the signals, localized voxels of >125 mm^3 were used rather than global scans, which meant that we could not compare the tumors to normal mammary glands, which are too small in volume. Thus, we compared the pH and pHLIP Var3 fluorescence detected in tumors to muscle (Fig. 4). Although muscle showed an overall pH of 7.1 ± 0.1 ($n = 3$) and no fluorescence signal above background levels, the pH measured in tumors of the same animal was lower at 6.7 ± 0.0 ($n = 3$), with a fluorescent signal over background ∼5.5 times higher than in background and 4.2 times higher than in muscle. The measured values represent bulk pH, with the pH at the surface of glycolytic cancer cells expected to be lower (53).

Our data clearly indicate correlations between tissue pH and pHLIP Var3 uptake and retention in vivo, raising questions of whether changes in pH might occur in early neoplasia and whether pHLIP Var3 will be able to reflect these changes. To examine early lesions, we used the transgenic BALB/neu-T model of breast cancer (48). These mice develop atypical mammary hyperplasia by week 9–10 of age, carcinoma in situ and invasive carcinoma around week 15, and palpable tumors between week 20 and 30. In our experiments, mice aged between 124 d and 151 d showed histological evidence of cancer and precursor hyperplasia. Because these lesions were relatively small, we could not detect the fluorescence after i.v. injection of pHLIP Var3 by whole animal

imaging; we could, however, reveal a signal after sacrifice and dissection (Fig. 5). We also examined older mice with palpable tumors. Eight breasts per animal were examined and dissected from each mouse, with a total of 164 samples taken. Histological sections from each breast were scored for the presence of hyperplasia, invasive carcinoma, necrosis, and whether any normal tissue was still retained within the sample. For each of these characteristics, we plotted a receiver–operator curve (ROC) of sensitivity versus specificity (Fig. 6). The fluorescent signal from the pHLIP Var3 peptide showed the highest sensitivity and specificity with regard to the presence or absence of invasive carcinoma, with an area under the ROC curve of 0.939 ± 0.028 SEM (Fig. 6*A* and Tables S2 and S3); less so for the presence of necrosis, with an area under the ROC curve of 0.860 ± 0.033 SEM (Fig. 6*B* and Tables S4 and S5); and less again for the retention of any normal tissue within the tumor, with an area under the ROC curve of 0.789 ± 0.041 SEM (Fig. 6*C* and Tables S6 and S7). We had wondered whether pHLIP Var3 retention was due to necrosis but found the correlation weaker than the correlation with carcinoma, confirming earlier findings that pHLIP Var3 did not target necrotic cores (54). Furthermore, we did not observe any signal in tissues without invasive carcinoma. We did not find any breasts with hyperplasia but without invasive cancer. Thus, there were no false-positives within our sample size (Table S2). Although large carcinomas (>5 mm GMD) were all positive for uptake, among the small but histological carcinomas, the results were variable. Fifty-seven percent of these were positive, an indication of a significant false-negative rate for early neoplastic lesions as assessed by pHLIP Var3.

Discussion

In this study we explored the feasibility of using the pHLIP Var3 peptide as a biomarker for detection of early neoplasia. Our data indicating that pHLIP Var3 exhibits tumor targeting and retention are in good accordance with previous findings with other
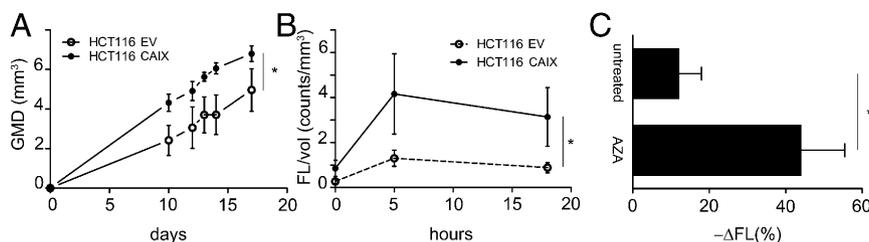
Fig. 3. pHLIP uptake and retention is pH dependent. (*A*) Tumor growth curves of EV and CAIX-overexpressing HCT116 cells in nude mice. CAIX overexpression enhanced tumor growth. (*B*) The uptake and retention of pHLIP Var3 in CAIX-overexpressing tumors (normalized to volume) was significantly higher than in EV controls over time. (*C*) AZA treatment reduced pHLIP retention significantly within 24 h. Mice bearing 4T1 tumors were injected with pHLIP and treated with AZA or left untreated. The mice were imaged at 1 h and 24 h postinjection, and the decline in fluorescence was calculated. The increase in pH as effected by AZA accelerated the decrease in pHLIP fluorescence significantly ($n = 4$–6 per group; data are mean ± SEM).
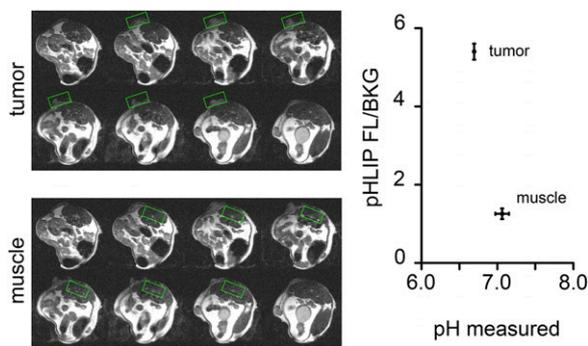
Fig. 4. The pH was measured in BALB/neu-T tumors in vivo. To demonstrate the feasibility of in vivo pH measurement, tumor-bearing BALB/neu-T mice were used in a 9.4T MRI tuned to the ^{31}P signal. To avoid contamination of the voxel measured, ISIS was used to specify the area of measurement. No fluorescence signal above background (FL/BKG) was detected from muscle, whereas the tumor showed a signal-to-noise ratio of ~2.5. At the same time, the tumor showed a lower pH of 6.7 ± 0.0 than the muscle, 7.1 ± 0.1 ($n = 3$ in both groups; data are mean $\pm$ SEM).

pHLIPs (24, 54). We show that manipulation of pH in spheroids and in xenografts by the use of CAIX-positive and -negative cancer cells leads to differential retention of pHLIP Var3, consistent with more acidic extracellular pH. The tuning of pH by AZA-mediated CAIX inhibition led to a significant decrease in pHLIP Var3 retention in 4T1 tumors. In previous work we showed that tumors from a variety of cancer types in mice retain pHLIP peptides (24, 37, 54). Here we have used both models of colorectal cancer and breast cancer. Thus, the retention of a signal from pHLIP Var3 peptide indicates the presence of extracellular acidosis in murine tumor models, and likely in man.

We then asked whether such a biomarker might be used to identify early neoplasia. Enhanced utilization of glycolytic metabolism is a characteristic, indeed hallmark, of cancer, however the time and extent of its induction during carcinogenesis are not known. Hence we examined the retention of pHLIP Var3 in a transgenic model of breast cancer. There was no evidence of retention of pHLIP Var3 in normal breast tissue. These results indicate that false-positives are uncommon in this model using pHLIP Var3 as a marker. And all of the larger cancers retained pHLIP Var3, indicative of acidic pH. Thus, detection of pHLIP Var3 appears to be a good indicator of well-established malignancy in this model as well. However, although most of the early lesions retained the pHLIP signal, many did not. This raises the intriguing possibility that lesions can be stratified based upon their pHLIP uptake, reflecting the extent of metabolic reprogramming in any given lesion. These results lead to the hypothesis that lesions with more acid pH may be more likely to go on to form progressive lesions. Although these experiments were done using an Alexa Fluor-conjugated version of pHLIP Var3, future studies in man could use single photon emission computed tomography (SPECT) or positron emission tomography (PET) tracers to enable detection. Fluorescence could possibly be useful for light imaging of dysplastic lesions of the gastrointestinal tract. Tumor pH may display heterogeneous distribution, affecting the overall signal; thus, pH imaging with higher spatial resolution might be needed to address this potential issue.

It is clear in human breast cancer that many lesions that appear to be cancerous by pathological criteria may not actually result in deleterious events for the patient. This is becoming apparent from the disappointing limitations of mammography to identify disease in patients that affects their long-term survival. Mammography clearly can recognize lesions that are identified by pathology as malignant. However, their removal has only a limited improvement on long-term survival of the population

overall (55, 56). Our results now raise the question of whether discrimination of lesional pH might add very valuable predictive information. Further research to determine whether altered pH in early neoplastic lesions correlates with biological behavior will be required and would help to possibly establish pH-based stratification of neoplastic lesions.

In conclusion, we believe that the pHLIPs, in general, and pHLIP Var3, specifically—with its significantly reduced level of false-positive signal—have the potential to be predictive markers of tumor invasiveness and aggressiveness.

Materials and Methods

Fig. 5. pHLIP Var3 detects spontaneously arising tumors in vivo. BALB/neu-T mice of different ages and therefore at different stages of tumor development were injected with pHLIP Var3. To measure the fluorescent signal from the tumors, mice were killed and the mammary glands/tumors were exposed (A). Late stage malignancies were highlighted by marked pHLIP uptake (c and d), whereas other regions in earlier stages of development in some cases were marked and in some cases were not marked (a and b). A total of 164 samples were taken and analyzed. (B) An example of a tumor showing invasive carcinoma (C) and carcinoma in situ (D).
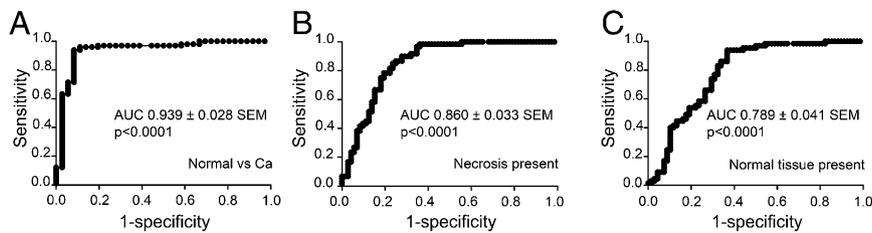
Fig. 6. ROC curves for pHLIP/IVIS measurements using (*A*) the presence of invasive carcinoma, (*B*) necrosis, or (*C*) normal tissue in the tumor samples. pHLIP Var3 was injected i.v. into BALB/neu-T mice at different stages of tumor development. A day later, the mammary glands were exposed to allow for measurement of fluorescence. Samples were then harvested and processed to compare the histopathology to the fluorescence readings. An invasive carcinoma was detected in 121 out of 164 samples, necrotic tissue was seen in 76 out of 161 samples, and normal tissue as well as carcinoma were present in 87 out of 162 samples. The fluorescence signal from the pHLIP Var3 peptide showed the best sensitivity and specificity for invasive carcinoma (*A*), less so for the presence of necrosis (*B*), and less again for the absence of normal tissue (*C*) in the tumors.

Charles River. BALB/neu-T mice (48) were bred by the biomedical services unit in Oxford.

In Vivo and Ex Vivo Animal Imaging. For in vivo measurements, animals were anesthetized and placed in an in vivo imaging system (IVIS; Xenogen). Alexa546 fluorescence was read (excitation, 500–550 nm; emission detected between 575 and 650 nm) and compared with a reading of background fluorescence, which was subtracted (Living Image software V3.2). The result was used to measure region of interest (ROI) fluorescence from the tumors. To visualize mammary glands in BALB/neu-T mice, mice were killed following pHLIP injection, the skin was removed, and tumors imaged in the IVIS. Mammary glands were harvested and one half snap-frozen in liquid nitrogen and the other half fixed in formalin for pathological evaluation.

Histopathology. Formalin-fixed paraffine-embedded samples were cut and stained with H&E. The samples were then graded by a pathologist blind to the experimental groups.

^{31}P MRS Measurement of pH in Vivo. MRS was performed on a 9.4 T 160 mm VNMRS horizontal bore preclinical imaging system equipped with a 100 mm bore gradient insert capable of 400 mT/m (Varian, Inc.). Radio frequency (RF) transmission was performed with an actively decoupled 35 mm ID quadrature birdcage coil (Rapid Biomedical GmbH). RF reception was performed with a custom-made actively decoupled 15 mm surface coil. ^{31}P localization was performed with image-selected in vivo spectroscopy (ISIS) (57) using

adiabatic hyperbolic secant inversion pulses with a bandwidth of 15 kHz in combination with outer voxel suppression. ^{31}P ISIS spectra from voxels (125–180 mm^3) placed within tumors were acquired with 1,024 averages from tumors and 256 averages from muscle and repetition time (TR) of 3 s. In the absence of detectable PCr signal, the α-ATP signal at −7.52 ppm was used as a chemical shift reference, as the α-ATP signal shift is virtually the same as that of the PCr signal in the pH range of 6–8 (58). Intracellular pH was calculated according to the chemical shift of the Pi signal using a modified Henderson–Hasselbach relationship with pK = 6.77, which represents average literature values (59).

Statistical Analysis. Unless stated otherwise, data are expressed as means ± SEM and were analyzed using the Mann–Whitney test for comparisons between two groups of animals and one-way ANOVA for more than two groups. *P* values lower than 0.05 were assumed to express a significant difference (*$P <$ 0.05, **$P <$ 0.01, ***$P <$ 0.001).

1. Vander Heiden MG, Cantley LC, Thompson CB (2009) Understanding the Warburg effect: The metabolic requirements of cell proliferation. *Science* 324(5930):1029–1033.
2. Cairns RA, Harris IS, Mak TW (2011) Regulation of cancer cell metabolism. *Nat Rev Cancer* 11(2):85–95.
3. Hanahan D, Weinberg RA (2011) Hallmarks of cancer: The next generation. *Cell* 144(5):646–674.
4. De Bock K, et al. (2013) Role of PFKFB3-driven glycolysis in vessel sprouting. *Cell* 154(3):651–663.
5. Damaghi M, Wojtkowiak JW, Gillies RJ (2013) pH sensing and regulation in cancer. Front Physiol 4:370.
6. Parks SK, Chiche J, Pouysségur J (2013) Disrupting proton dynamics and energy metabolism for cancer therapy. *Nat Rev Cancer* 13(9):611–623.
7. Wykoff CC, et al. (2000) Hypoxia-inducible expression of tumor-associated carbonic anhydrases. *Cancer Res* 60(24):7075–7083.
8. McIntyre A, et al. (2012) Carbonic anhydrase IX promotes tumor growth and necrosis in vivo and inhibition enhances anti-VEGF therapy. *Clin Cancer Res* 18(11):3100–3111.
9. Swietach P, Patiar S, Supuran CT, Harris AL, Vaughan-Jones RD (2009) The role of carbonic anhydrase 9 in regulating extracellular and intracellular ph in three-dimensional tumor cell growths. *J Biol Chem* 284(30):20299–20310.
10. Kallinowski F, Vaupel P (1988) pH distributions in spontaneous and isotransplanted rat tumours. *Br J Cancer* 58(3):314–321.
11. Vaupel P, Kallinowski F, Okunieff P (1989) Blood flow, oxygen and nutrient supply, and metabolic microenvironment of human tumors: A review. *Cancer Res* 49(23):6449–6465.
12. Gerweck LE, Seetharaman K (1996) Cellular pH gradient in tumor versus normal tissue: Potential exploitation for the treatment of cancer. *Cancer Res* 56(6):1194–1198.
13. Bhujwalla ZM, et al. (2002) Combined vascular and extracellular pH imaging of solid tumors. *NMR Biomed* 15(2):114–119.
14. Gatenby RA, Gawlinski ET, Gmitro AF, Kaylor B, Gillies RJ (2006) Acid-mediated tumor invasion: A multidisciplinary study. *Cancer Res* 66(10):5216–5223.
15. Iessi E, Marino ML, Lozupone F, Fais S (2008) Tumor acidity and malignancy: Novel aspects in the design of anti-tumor therapy. *Cancer Ther* 6(1):55–66.

16. Gillies RJ, Verduzco D, Gatenby RA (2012) Evolutionary dynamics of carcinogenesis and why targeted therapy does not work. *Nat Rev Cancer* 12(7):487–493.
17. Martínez-Zaguilán R, et al. (1996) Acidic pH enhances the invasive behavior of human melanoma cells. *Clin Exp Metastasis* 14(2):176–186.
18. Rofstad EK, Mathiesen B, Kindem K, Galappathi K (2006) Acidic extracellular pH promotes experimental metastasis of human melanoma cells in athymic nude mice. *Cancer Res* 66(13):6699–6707.
19. Kato Y, et al. (2005) Acidic extracellular pH induces matrix metalloproteinase-9 expression in mouse metastatic melanoma cells through the phospholipase D-mitogen-activated protein kinase signaling. *J Biol Chem* 280(12):10938–10944.
20. Robey IF, et al. (2009) Bicarbonate increases tumor pH and inhibits spontaneous metastases. *Cancer Res* 69(6):2260–2268.
21. Hashim AI, Zhang X, Wojtkowiak JW, Martinez GV, Gillies RJ (2011) Imaging pH and metastasis. *NMR Biomed* 24(6):582–591.
22. Lee ES, Gao Z, Bae YH (2008) Recent progress in tumor pH targeting nanotechnology. *J Control Release* 132(3):164–170.
23. Nwe K, Huang C-H, Tsourkas A (2013) Gd-labeled glycol chitosan as a pH-responsive magnetic resonance imaging agent for detecting acidic tumor microenvironments. *J Med Chem* 56(20):7862–7869.
24. Weerakkody D, et al. (2013) Family of pH (low) insertion peptides for tumor targeting. *Proc Natl Acad Sci USA* 110(15):5834–5839.
25. Andreev OA, Reshetnyak YK (2014) Targeting diseased tissues by pHLIP insertion at low cell surface pH. *Front Physiol* 5:97.
26. Reshetnyak YK, Andreev OA, Lehnert U, Engelman DM (2006) Translocation of molecules into cells by pH-dependent insertion of a transmembrane helix. *Proc Natl Acad Sci USA* 103(17):6460–6465.
27. Wijesinghe D, Engelman DM, Andreev OA, Reshetnyak YK (2011) Tuning a polar molecule for selective cytoplasmic delivery by a pH (low) insertion peptide. *Biochemistry* 50(47):10215–10222.
28. An M, Wijesinghe D, Andreev OA, Reshetnyak YK, Engelman DM (2010) pH-(low)-insertion-peptide (pHLIP) translocation of membrane impermeable phalloidin toxin inhibits cancer cell proliferation. *Proc Natl Acad Sci USA* 107(47):20246–20250.

29. Moshnikova A, Moshnikova V, Andreev OA, Reshetnyak YK (2013) Antiproliferative effect of pHLIP-amanitin. *Biochemistry* 52(7):1171–1178.
30. Wijesinghe D, Arachchige MCM, Lu A, Reshetnyak YK, Andreev OA (2013) pH dependent transfer of nano-pores into membrane of cancer cells to induce apoptosis. Sci Rep 3:3560.
31. Segala J, Engelman DM, Reshetnyak YK, Andreev OA (2009) Accurate analysis of tumor margins using a fluorescent pH Low Insertion Peptide (pHLIP). *Int J Mol Sci* 10(8): 3478–3487.
32. Vāvere AL, et al. (2009) A novel technology for the imaging of acidic prostate tumors by positron emission tomography. *Cancer Res* 69(10):4510–4516.
33. Andreev OA, Engelman DM, Reshetnyak YK (2009) Targeting acidic diseased tissue: New technology based on use of the pH (Low) Insertion Peptide (pHLIP). *Chim Oggi* 27(2):34–37.
34. Macholl S, et al. (2012) In vivo pH imaging with (99m)Tc-pHLIP. *Mol Imaging Biol* 14(6):725–734.
35. Daumar P, et al. (2012) Efficient (18)F-labeling of large 37-amino-acid pHLIP peptide analogues and their biological evaluation. Bioconjug Chem 23(8):1557–1566.
36. Yao L, et al. (2013) pHLIP peptide targets nanogold particles to tumors. *Proc Natl Acad Sci USA* 110(2):465–470.
37. Cruz-Monserrate Z, et al. (2014) Targeting pancreatic ductal adenocarcinoma acidic microenvironment. *Sci Rep* 4:4410.
38. Viola-Villegas NT, et al. (2014) Understanding the pharmacological properties of a metabolic PET tracer in prostate cancer. *Proc Natl Acad Sci USA* 111(20):7254–7259.
39. Sosunov EA, et al. (2013) pH (low) insertion peptide (pHLIP) targets ischemic myocardium. *Proc Natl Acad Sci USA* 110(1):82–86.
40. Li N, et al. (2013) Peptide targeting and imaging of damaged lung tissue in influenza-infected mice. *Future Microbiol* 8(2):257–269.
41. Han L, et al. (2013) pH-controlled delivery of nanoparticles into tumor cells. *Adv Healthc Mater* 2(11):1435–1439.
42. Zhao Z, et al. (2013) A controlled-release nanocarrier with extracellular pH value driven tumor targeting and translocation for drug delivery. *Angew Chem Int Ed Engl* 52(29):7487–7491.
43. Davies A, Lewis DJ, Watson SP, Thomas SG, Pikramenou Z (2012) pH-controlled delivery of luminescent europium coated nanoparticles into platelets. *Proc Natl Acad Sci USA* 109(6):1862–1867.
44. Yao L, Daniels J, Wijesinghe D, Andreev OA, Reshetnyak YK (2013) pHLIP®-mediated delivery of PEGylated liposomes to cancer cells. *J Control Release* 167(3):228–237.
45. Reshetnyak YK, et al. (2011) Measuring tumor aggressiveness and targeting metastatic lesions with fluorescent pHLIP. *Mol Imaging Biol* 13(6):1146–1156.
46. Loja MN, et al. (2013) Optical molecular imaging detects changes in extracellular pH with the development of head and neck cancer. *Int J Cancer* 132(7):1613–1623.
47. Luo Z, et al. (2014) Widefield optical imaging of changes in uptake of glucose and tissue extracellular pH in head and neck cancer. *Cancer Prev Res (Phila)* 7(10):1035–1044.
48. Boggio K, et al. (1998) Interleukin 12-mediated prevention of spontaneous mammary adenocarcinomas in two lines of Her-2/neu transgenic mice. *J Exp Med* 188(3):589–596.
49. Dubois L, et al. (2011) Specific inhibition of carbonic anhydrase IX activity enhances the in vivo therapeutic effect of tumor irradiation. *Radiother Oncol* 99(3):424–431.
50. Gillies RJ, Liu Z, Bhujwalla Z (1994) 31P-MRS measurements of extracellular pH of tumors using 3-aminopropylphosphonate. *Am J Physiol* 267(1 Pt 1):C195–C203.
51. Stubbs M, et al. (1992) An assessment of 31P MRS as a method of measuring pH in rat tumours. *NMR Biomed* 5(6):351–359.
52. Evelhoch JL, Sapareto SA, Jick DE, Ackerman JJ (1984) In vivo metabolic effects of hyperglycemia in murine radiation-induced fibrosarcoma: A 31P NMR investigation. *Proc Natl Acad Sci USA* 81(20):6496–6500.
53. Chiche J, Brahimi-Horn MC, Pouysségur J (2010) Tumour hypoxia induces a metabolic shift causing acidosis: A common feature in cancer. *J Cell Mol Med* 14(4):771–794.
54. Adochite R-C, et al. (2014) Targeting breast tumors with pH (low) insertion peptides. *Mol Pharm* 11(8):2896–2905.
55. Marmot MG, et al. (2012) The benefits and harms of breast cancer screening: An independent review. *Lancet* 380(9855):1778–1786.
56. Welch HG, Passow HJ (2014) Quantifying the benefits and harms of screening mammography. *JAMA Intern Med* 174(3):448–454.
57. Ordidge R, Connelly A, Lohman JA (1986) Image-selected in vivo spectroscopy (ISIS). A new technique for spatially selective nmr spectroscopy. *J Magn Reson* 66(2):283–294.
58. Moon RB, Richards JH (1973) Determination of intracellular pH by 31P magnetic resonance. *J Biol Chem* 248(20):7276–7278.
59. De Graaf RA (2007) In Vivo NMR Spectroscopy: Principles and Techniques (John Wiley & Sons, Chichester, UK), 2nd Ed.

MEDICAL SCIENCES